

## Superconductivity in Palladium Hydride Systems

Kawae, Tatsuya

Department of Applied Quantum Physics, Faculty of Engineering, Kyushu University

Inagaki, Yuji

Department of Applied Quantum Physics, Faculty of Engineering, Kyushu University

Wen, Si

Department of Applied Quantum Physics, Faculty of Engineering, Kyushu University

Hirota, Souhei

Department of Applied Quantum Physics, Faculty of Engineering, Kyushu University

他

<https://hdl.handle.net/2324/7172285>

---

出版情報 : Journal of the Physical Society of Japan. 89 (5), pp.051004-1-051004-10, 2020-02-25.

日本物理学会

バージョン :

権利関係 : Creative Commons Attribution 4.0 International





## Superconductivity in Palladium Hydride Systems

Tatsuya Kawae<sup>1,3\*</sup>, Yuji Inagaki<sup>1,3</sup>, Si Wen<sup>1</sup>, Souhei Hirota<sup>1</sup>, Daiki Itou<sup>2</sup>, and Takashi Kimura<sup>2,3</sup>

<sup>1</sup>Department of Applied Quantum Physics, Faculty of Engineering, Kyushu University, Fukuoka 819-0395, Japan

<sup>2</sup>Department of Physics, Faculty of Science, Kyushu University, Fukuoka 819-0395, Japan

<sup>3</sup>Research Center for Quantum Nano-Spin Sciences, Kyushu University, Fukuoka 819-0395, Japan

(Received October 1, 2019; accepted December 9, 2019; published online February 25, 2020)

The superconductivity of palladium–hydride (Pd–H) system was discovered by Skoskiewicz in 1972. Thereafter, many studies have been carried out on Pd–H and palladium deuteride (Pd–D) systems along with their alloyed (Pd–metal–H) systems. In this paper, we present a brief overview of superconducting properties of these systems. First, we describe methods for H loading into Pd, in which three principal techniques, i.e., gas loading, electrochemical loading, and H implantation are introduced. Next, we briefly summarize the superconducting properties of Pd–H(D) systems, e.g., the concentration dependence of the transition temperature  $T_c$ , inverse isotope effect, critical field, pressure dependence of  $T_c$ , and the impurity effects. Subsequently, we describe our recent in-situ magnetization measurements of superconducting Pd–H and Pd–D powders with 1–2  $\mu\text{m}$  diameters prepared by low-temperature H absorption, in which the absorption was performed below 200 K under hydrogen ( $\text{H}_2$ ) or deuterium ( $\text{D}_2$ ) gas atmosphere. Additionally, we report resistance measurements of a Pd–H film with  $\sim 100$  nm thickness prepared by the same H absorption procedure. The superconducting transition temperature of the film is consistent with that of the powders. From these results, we conclude that the low-temperature H absorption method is useful for preparing high quality Pd–H and Pd–D samples.

### 1. Introduction

Great attention has been focused on research into superconductivity in hydrogen (H) rich materials, owing to the recent discovery of new superconductors, such as sulfur hydride and lanthanum hydride with transition temperatures  $T_c$  higher than  $\sim 200$  K.<sup>1,2</sup> Theoretical predictions pointed out the possibility of high transition temperatures,  $T_c$ , in many hydrogen-rich materials once these are pressurized up to a few hundred GPa.<sup>3</sup> However, experimental investigations exploring the microscopic nature of the origin of superconductivity are difficult under such extreme conditions. In contrast, palladium hydride ( $\text{PdH}_x$  where  $x = \text{H}/\text{Pd}$ ) exhibits superconductivity under ambient pressure, thereby enabling the study of superconducting properties through a variety of measurements. This suggests that the Pd–H system is a good material to investigate the role of H in the occurrence of superconductivity in hydride systems, which would give a clue for discovering a new hydride superconductor with a high transition temperature.

The first investigation of superconducting metal hydrides was reported by Horn and Ziegler in 1947,<sup>4</sup> where the superconducting transition temperatures  $T_c$  in tantalum and niobium hydrides were suppressed as compared to those before hydrogenation. In contrast, an increase of  $T_c$  was reported in the thorium (Th) hydride system in 1970. Satterthwaite and Toepke found that  $\text{Th}_4\text{H}_{15}$  exhibits a superconducting transition at  $\sim 8$  K,<sup>5</sup> which is much higher than  $T_c = 1.37$  K for pure Th. After that, the Pd–H system, which is the best-known superconducting hydride, and the Pd–metal–H alloy system were reported to exhibit superconductivity by Skoskiewicz in 1972,<sup>6</sup> where onset temperatures of above  $\sim 4$  K were found at a composition  $\text{PdH}_{0.87}$  and Pd–nickel (Ni)(1.5%)– $\text{H}_{0.84}$ . These findings sparked numerous investigations on hydrides.

In this paper, we briefly summarize previous experimental investigations on superconducting  $\text{PdH}_x$  and Pd deuteride ( $\text{PdD}_x$ ) and report our recent studies. First, we describe the representative ways for H and D charging into Pd, in which

three methods, i.e., gas loading, electrochemical loading, and H implantation are introduced. Next, we present a brief overview of the superconducting properties of  $\text{PdH}_x$  and  $\text{PdD}_x$ . Finally, we show our recent in-situ magnetization measurements of superconducting  $\text{PdH}_x$  and  $\text{PdD}_x$  powders and resistance measurements of a  $\text{PdH}_x$  film prepared by low-temperature H absorption.

### 2. Hydrogen Charging in Palladium

In metallic hydrides, H atoms occupy the interstitial sites in the metal lattices. Therefore, a nonstoichiometric composition between the host metal and the H atom extends into the  $x$ – $P$ – $T$  phase diagram, where  $x$ ,  $P$ , and  $T$  are the ratio of the H concentration to host metal  $M$ , i.e.,  $x = \text{H}/M$ , pressure, and temperature, respectively. Figure 1 illustrates the  $x$ – $P$ – $T$  phase diagram of  $\text{PdH}_x$ .<sup>7</sup> It is well known that Pd metal can absorb high numbers of H atoms even at room temperature. When a Pd metal with an fcc cubic structure is exposed to a  $\text{H}_2$  gas atmosphere, the  $\text{H}_2$  molecule is dissociated into two H atoms on the Pd surface, which are then absorbed into the interstitial sites of the Pd lattice. As a result of the absorption, two different phases,  $\alpha$  and  $\beta$ , emerge in the phase diagram. At around room temperature ( $\sim 300$  K), the  $\alpha$  phase is stable up to  $x \sim 0.02$ , where the Pd lattice expands slightly from 0.389 to 0.390 nm.<sup>8</sup> The  $\beta$  phase, with a lattice constant with 0.402 nm is stable above  $x \sim 0.61$ . Both phases coexist between  $0.02 \leq x \leq 0.61$ .

Under a  $\text{H}_2$  gas pressure of 1 atm, the H concentration for  $\text{PdH}_x$  is increased to  $x \sim 0.7$  at room temperature, as displayed in Fig. 1. However, this concentration is lower than the critical concentration for the superconductivity in  $\text{PdH}_x$ , meaning that a different procedure is necessary to increase the H concentration further to be able to observe superconductivity.

Here, three principal methods, i.e., loading from high pressure gas, electrochemical loading, and ion implantation, will be presented, which have been widely used to synthesize highly concentrated samples with  $x > 0.75$ . In contrast to the easy uptake of H atoms in Pd, it is difficult to keep the highly



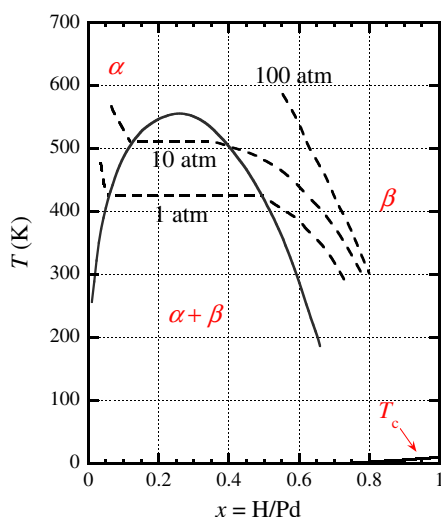


**Fig. 1.** (Color online) The H concentration–pressure–temperature ( $x$ – $P$ – $T$ ) phase diagram of Pd–H systems.<sup>7)</sup> The H concentration in Pd ( $x = \text{H}/\text{Pd}$ ) is increased with decreasing temperature at the same H pressure. The superconductivity appears at a H concentration of above  $x \sim 0.75$ .

concentrated H state after H charging, because Pd metals easily desorb H atoms. Hence, we must pay special attention to preventing H desorption during the sample mounting on a cryostat after the H charging, which is crucial for exploring superconducting properties in  $\text{PdH}_x$  and  $\text{PdD}_x$ .

### 2.1 Loading from gas phase

A highly concentrated H sample was obtained using a high-pressure experimental setup in which Pd is exposed to pressurized  $\text{H}_2$  gas, as can be seen in the phase diagram of  $\text{PdH}_x$  in Fig. 1. The experiments were performed using the following procedure. The Pd sample was mounted in a high-pressure cell and pressurized with  $\text{H}_2$  gas at room temperature, by introducing  $\text{H}_2$  gas through a capillary. After waiting sufficiently long for H loading into Pd to happen, the pressure cell was cooled to liquid  $\text{N}_2$  temperature (77 K) to keep the H concentration in Pd constant. Subsequently, the superconducting properties were measured. Using this method, Shirber and co-workers obtained ratios of  $\text{H}/\text{Pd} = 0.97$  and  $\text{D}/\text{Pd} = 0.95$  under a  $\text{H}_2$  pressure of 4–5 kbar.<sup>9,10)</sup> Additionally, they succeeded in preparing palladium-tritide ( $\text{PdT}_x$ ) system and measuring its  $T_c$ , which is higher than that of  $\text{PdH}_x$  and  $\text{PdD}_x$  with the same H concentration.<sup>11)</sup> In this method, the H concentration is estimated from the change in the gas pressure in a reference volume using Sieverts technique<sup>12)</sup> and/or from the change in the sample weight.<sup>13)</sup>

Many experimental studies have been performed in Pd–H, Pd–D, and Pd–metal–H systems using the high-pressure gas absorption method.<sup>13–19)</sup> Importantly, Hemmes et al. synthesized stoichiometric PdH and PdD under very high pressures of  $\text{H}_2$  or  $\text{D}_2$  sealed in a diamond-anvil cell (DAC). After filling the DAC with liquid  $\text{H}_2$  or  $\text{D}_2$ , the cell was heated to a temperature sufficient for H (D) absorption and diffusion into the sample metal, where the hydrogen pressure was reached at  $\sim 4$  GPa.<sup>20–22)</sup>

### 2.2 Electrochemical loading

Electrochemical loading can easily achieve a high H concentration, which is above the critical concentration for

superconductivity and without the use of a high-pressure environment. This can be understood by looking at the reaction as an equilibrium between H in the electrochemical phase and H in the solid phase. Skoskiewicz loaded H into Pd and Pd–Ni alloys with a H concentration of  $x \sim 0.95$  by electrolysis of  $0.1\text{N-H}_2\text{SO}_4$  at current densities of 50 to  $150 \text{ mA}/\text{cm}^2$ , with Pt leads spot-welded to the sample.<sup>6,23)</sup> By decreasing the loading temperature to  $\sim 190$  K, a H concentration with  $x \sim 1$  was achieved, enabling many experimental studies on Pd–H systems in the highly concentrated region.<sup>24–32)</sup> An electrolytic solution of  $\text{H(D)Cl}$  in  $\text{CH}_3\text{OH(D)}$  was also used for H and D loading, allowing for the comparison of the superconducting properties of Pd–H and Pd–D systems.<sup>33–40)</sup> The H concentration in the sample was determined by weighing the sample after H loading and/or measuring the gas volume after H desorption from the sample.

After H loading, the sample was rapidly cooled to 77 K to prevent H transport. Nevertheless, H atoms inevitably left the sample while mounting the sample on the cryostat, which leads to inhomogeneity of the H concentration in the sample and, as a result, a broadening of the superconducting transition.

### 2.3 Ion implantation

The implantation of H into  $\text{PdH}_x$ , was carried out at 4 K to stabilize the implanted H. The average penetration depth of the H ions was about  $1 \mu\text{m}$  at a  $\text{H}_2^+$  beam energy of 130 keV, resulting in a high concentration layer of implanted H over a thickness of some hundreds of nm thick of the Pd foil.<sup>41)</sup> Before the implantation, the foil was pre-charged with H (or D) under  $\text{H}_2$  ( $\text{D}_2$ ) gas at high temperature to shorten the implantation time, by which  $x \sim 0.7$  was obtained. The foil was then quickly cooled to 77 K to minimize the loss of H prior to implantation.

As described above, H atoms are charged with the same density for only a narrow region in the specimen as far as the constant energy implantation is utilized, implying that the spatial inhomogeneity of H content is inevitable. In addition, the ion implantation is accompanied by damage of the sample as the kinetic energy of the ions dissipates in collisions. This causes atomic displacements, which induce vacancies and voids. Hence, a broad superconducting transition was observed in the samples prepared using this method.<sup>41)</sup>

Nevertheless, it should be noted that H implantation is quite a powerful method, because the H concentration in a host metal can be increased up to a non-equilibrium region by injecting H atoms at low temperatures, at which H atoms are not released from the metal. Actually, this method has been applied to many alloys with a low H solubility.<sup>42–47)</sup>

## 3. Superconducting Properties of Pd–H System

### 3.1 Magnetic susceptibility of Pd–H system

After the discovery of the superconductivity in  $\text{PdH(D)}_x$ , many experimental studies have been carried out, revealing the following features of the superconductivity of Pd–H(D) systems. However, before summarizing the superconducting properties, we briefly explain the magnetic properties of Pd in the normal region. Pd metal is an enhanced Pauli paramagnet with strong spin fluctuations, which suppress the formation of Cooper pair according to the BCS theory. Therefore, its vanishing paramagnetism is considered to be the necessary

precondition for the occurrence of superconductivity in Pd–H(D) systems.<sup>48)</sup>

The magnetic susceptibility of Pd–H system shows a large variation with H concentration  $x$ .<sup>49)</sup> In the  $\alpha$  phase, the enhanced paramagnetic susceptibility is approximately independent of  $x$  because the Fermi surface of the  $\alpha$  phase is almost the same as that of pure Pd. In contrast, the susceptibility of the  $\beta$  phase is calculated to be a small positive value, as the  $d$ -band is filled by  $s$  electrons. Hence, in the  $\alpha$ – $\beta$  mixed phase, for  $0.02 \leq x \leq 0.61$  at room temperature, the susceptibility decreases rapidly with increasing  $x$ . Note that the susceptibility was observed to be slightly negative, i.e., diamagnetic, and almost independent of  $x$ , in the magnetic susceptibility measurements of the  $\beta$  phase. This is caused by the addition of the diamagnetic contribution of the core electrons to the susceptibility in the  $\beta$  phase. These results indicate that the superconductivity occurs in the region where the spin fluctuations in pure Pd are suppressed. The above scenario is confirmed by our experiments through in-site magnetization measurements in PdH(D) <sub>$x$</sub> , as will be described later.

### 3.2 $T_c$ dependence on H concentration

Figure 2 shows plots of the concentration dependence of the superconducting transition temperature. The critical concentration for superconductivity was estimated to be  $x \sim 0.72$  for PdH <sub>$x$</sub>  and  $x \sim 0.67$  for PdD <sub>$x$</sub> .<sup>39)</sup> The maximum of  $T_c$  was observed at around 9 K for Pd–H and 11 K for Pd–D systems, respectively, which were achieved at a stoichiometric concentration of  $x = 1$ .<sup>20,34,39)</sup> According to Standley et al.,  $T_c(0)$  is given empirically by the relation  $T_c(0) = 150.8(x - x_0)^{2.244}$ , where  $x_0 = 0.715$  and  $0.668$  for the H and D systems, respectively.<sup>39)</sup> At the same  $x$  concentration for H and D,  $T_c$  in the H system is lower than that in the D system, which is known as the inverse isotope effect.<sup>13,34,50)</sup>

### 3.3 Pressure effect on $T_c$

The pressure dependence of the superconducting transition temperature  $T_c$  of PdH <sub>$x$</sub>  and PdD <sub>$x$</sub>  has been studied by several groups. Their samples were prepared by the gas loading and the electrochemical reaction.<sup>9,13,20,24)</sup> The results show a negative pressure effect, so that increasing the pressure on PdH(D) <sub>$x$</sub>  suppresses  $T_c$ . Moreover, the magnitude of the suppression is enhanced when the transition temperature is lowered with decreasing the concentration  $x$  at ambient pressure, as depicted in Fig. 2. The decrease of  $T_c$  with increasing pressure can be understood by a hardening of the phonon spectrum, causing a decrease of the electron–phonon-coupling constant  $\lambda$ . The negative pressure effect contradicts the theoretical assumption that a superconducting metallic hydrogen sublattice emerges inside the Pd lattice,<sup>51)</sup> because a smaller H–H distance should be more favorable for superconductivity.

Hemmes et al. explained the pressure dependence of  $T_c$  not only in the stoichiometric PdH and PdD but also in the substoichiometric samples based on their experimental results for the stoichiometric hydrides using DAC and band-structure calculations.<sup>20)</sup> According to them, the anharmonicity and the Debye–Waller factor play an important role for the inverse isotope effects and the pressure dependence of  $T_c$  in the Pd–H(D) system.

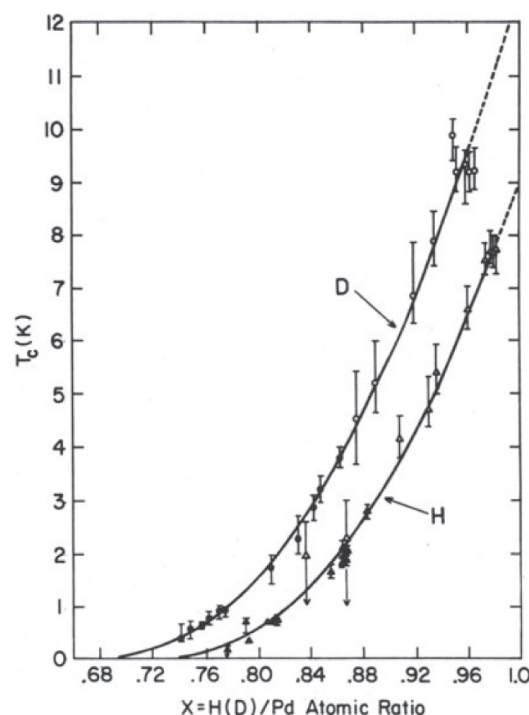


Fig. 2.  $T_c$  as a function of H(D) concentration for hydrogenated and deuterated Pd. This figure is taken from Ref. 39. © 1979 ELSEVIER.

### 3.4 Critical field

There has been a discrepancy of the superconducting critical fields between experiments, as follows. Skoskiewicz showed that the upper critical field  $H_{c2}$  is 1800 Oe,<sup>23)</sup> while Alekseevskii et al. reported  $H_{c2} = 2500$  Oe.<sup>25)</sup> In these experiments,  $H_{c2}$  were independent of the H concentration. In contrast, Krahn reported a concentration dependence of  $H_{c2}$ , which increased linearly with decreasing temperature over a wide temperature range.<sup>38)</sup> According to magnetization measurements, PdH <sub>$x$</sub>  for  $x$  much smaller than 1 is a type II superconductor,<sup>14)</sup> suggesting that the upper critical field  $H_{c2}(0)$  at  $T = 0$  K depends strongly on the mean free path of the electrons, i.e., on lattice distortions and impurities. This might be the reason why different  $H_{c2}$  values have been reported.

McLachlan et al. measured the temperature dependence of the magnetization of PdH <sub>$x$</sub>  at  $x \sim 1$  and concluded that a stoichiometric Pd–H is a type I superconductor.<sup>31)</sup> Moreover, Skoskiewicz et al. reported that a homogeneous PdH <sub>$x$</sub>  is a type I superconductor.<sup>16)</sup> In a homogeneous sample, the mean free path of the conduction electrons increases. Consequently, the coherence length increases and the penetration depth decreases, which might result in the emergence of a type I superconductor.

### 3.5 Other experiments on the Pd–H system

The electronic specific heat coefficient  $\gamma$ , which reflects the electronic density of state, is 9.5 mJ/(mol·K<sup>2</sup>) for pure Pd and decreases when small amounts of H are added.<sup>52)</sup> For the superconducting region between  $x = 0.83$  and  $0.88$ , Mackliet et al. reported that  $\gamma$  in the normal region is about six times smaller than that in pure Pd.<sup>26,27)</sup> Moreover, Zimmermann et al. measured the specific heat at  $x = 0.96$ .<sup>35)</sup> However, a broadening of the superconducting transition was observed,



which could be caused by a macroscopic compositional inhomogeneity in the samples. Thus there might be a large uncertainty in the determination of  $\gamma$  at  $x = 0.96$ .

A detailed discussion on neutron-scattering experiments is given in another paper in this issue, so that only the essential results related to superconductivity are summarized here. The lattice dynamics of a single crystal of  $\text{PdD}_{0.63}$  were studied by Rowe et al.,<sup>53)</sup> in which the acoustic mode frequencies were found to be 20% lower than those of pure Pd. This decrease was about four times larger than the expected value for the expanded lattice,<sup>54)</sup> suggesting that H charging brings about softening of the acoustic phonons. Based on the incoherent neutron scattering results of polycrystalline samples of  $\text{PdH}_{0.63}$ , the Pd–H force constants are considered to be about 20% stronger than the corresponding Pd–D force constants.<sup>55,56)</sup> This anharmonicity is believed to be the main reason for the occurrence of the inverse isotope effect in the superconductivity in Pd–H(D) systems.<sup>57)</sup>

Tunneling experiments for the direct observation of the tunnel gap on the Fermi surface have been carried out in the Pd–H(D) and Pd–Ni–H systems by several groups.<sup>47,58–61)</sup> The basic configuration of the experimental device consists of an Al–oxide–(Pd–H) tunnel junction. After depositing an Al film on a substrate, its surface was oxidized to form the tunnel barrier and Pd was evaporated onto the film. To avoid the destruction of the tunnel junction by the increase of the lattice constant due to H(D) absorption, the charging procedures were well designed.

The current–voltage ( $I$ – $V$ ) characteristics and their first and second derivatives were measured as a function of the voltage applied to the junctions. The superconducting energy gap  $\Delta$  was measured directly from the first derivative of the differential conductance  $dI/dV$ . The ratio  $2\Delta/k_B T_c$  for  $T_c$  between 4.6 and 7.5 K was observed at around 3.7, indicating that Pd–H and Pd–D are medium coupling superconductors in the concentration range investigated in these experiments. From the second derivative  $d^2I/dV^2$ , the quantity of the electron–phonon coupling  $\alpha^2(\omega)F(\omega)$  can be derived with the help of the Eliashberg equations. The structures in  $d^2I/dV^2$  spectra suggest that the optical phonon mode plays an important role in the superconductivity.

### 3.6 Superconducting properties of Pd alloy system

The inverse isotope effect observed in  $\text{PdH(D)}_x$  raises the question of whether  $T_c$  continues to increase with increasing mass of the interstitial element. To answer this question, boron (B), carbon (C), and nitrogen (N) were implanted in Pd by Stritzker and Becker,<sup>62–64)</sup> all of which lowered the  $T_c$ . This can be understood by considering the change in the electronic structure resulting from adding these elements. H and D enhance the electron–phonon coupling due to the screening of protons and deuterons by the conduction electrons. With heavier elements such as B, C, and N, in contrast, this coupling would be reduced because the nuclei are more effectively screened by their core electrons. Consequently, the electron–phonon coupling is lowered.

Substitution of Pd by other elements changes the electronic structure and phonon spectrum of the host system, and consequently leads to the shift of  $T_c$  compared to that of  $\text{PdH}_x$ . By using H implantation at low temperatures and thereby enabling the achievement of non-equilibrium H

concentrations, the H concentration dependence of  $T_c$  in the Pd alloy system,  $\text{Pd}_{1-y}\text{M}_y\text{H}_x$ , was studied.<sup>47)</sup> With the substitution of neighboring elements platinum (Pt), Ni, and rhodium (Rh), the following results were reported. With Pt,  $T_c$  was not affected much by a substitution of up to  $y \sim 0.25$ . With Ni and Rh substitution,  $T_c$  was suppressed with an increasing number of substituted atoms. With noble metals, copper (Cu), silver (Ag), and gold (Au), an increase of  $T_c$  was observed. The maximums of  $T_c$  were reported to be observed at  $\sim 17$  K with Cu at  $y = 0.45$ , at  $\sim 16$  K with Ag at  $y = 0.30$ , and at  $\sim 14$  K with Au at  $y = 0.16$ , respectively. It seems that the electronic properties of the host lattice does not play an important role in the superconductivity of the hydrogenated alloy.<sup>47)</sup>

In contrast, for Pd alloy prepared by gas loading or electrochemical reaction, quite different results were reported. With Ni substitution, a scatter of the transition temperature, i.e., a decrease and an increase of  $T_c$  were observed with increasing Ni concentration.<sup>6,65)</sup> With Cu, Ag, Rh, Pt, and Au substitution,  $T_c$  was suppressed with increasing numbers of substituted atoms.<sup>18,66–69)</sup> In the case of Nb substitution, which is a H absorption metal, an increase of  $T_c$  was reported.<sup>70)</sup> These results imply that the substitutions reduce the H solubility considerably,<sup>7)</sup> and consequently, in comparison to pure Pd, it would be very difficult to increase the H concentration in Pd alloys by gas loading or electrochemical reaction.

Substitutions other than the transition element were also performed with silicon (Si), aluminum (Al), and indium (In). In  $\text{Pd}_{1-y}\text{Si}_y$  alloys loaded with H by implantation at low temperatures, the superconducting properties in the amorphous region ( $0.17 \leq y \leq 0.20$ ) were similar to those in the f.c.c lattice region ( $0 \leq y \leq 0.05$ ), indicating that the influence of the lattice structure on superconductivity in the Pd–H system is minor.<sup>63,64)</sup> In  $\text{Pd}_{1-y}\text{Al}_y$  and  $\text{Pd}_{1-y}\text{In}_y$  alloys charged by H implantation, a slight increase of  $T_c$  was observed at  $y \sim 0.07$ .<sup>71)</sup> At Al and In concentration larger than  $y \sim 0.1$ ,  $T_c$  decreased with increasing their concentrations.

## 4. Low-Temperature Hydrogen Absorption

Numerous theoretical studies have been devoted to understanding the superconductivity of  $\text{PdH(D)}_x$  systems over the last decades.<sup>34,48,51,57,72–91)</sup> However, the number of experimental studies on superconductivity in  $\text{PdH(D)}_x$  were decreased rapidly after the late 1980's, although unresolved problems such as the origin of the inverse isotope effect and the concentration dependence of the critical field have remained, as mentioned above. This is because significant attention has been paid to high- $T_c$  cuprate superconductors after their discovery in the late 1980's. In addition, difficulties in the preparation of high quality hydride samples should be considered. The following three principal methods have been used for highly concentrated H loading into Pd to explore the superconducting properties. In the gas loading method, the superconducting transition was investigated in a specially designed pressure cell. In the electrochemical loading, the desorption of H was inevitable during the sample mounting in the cryostat. In the ion implantation, the spatial inhomogeneity of H (D) brings about a broadening of the transition.

We demonstrated a new method to study the superconducting properties of  $\text{PdH}(\text{D})_x$ , in which H (D) atoms are loaded into Pd at low temperature, much lower than room temperature.<sup>92,93)</sup> Although this method is based on gas loading, a high-pressure cell is not necessary for the loading, meaning that the procedure is much easier as compared to the previous methods and enables in-situ measurements. The temperature dependence of the H concentration  $x$ , given in Fig. 1, shows that the equilibrium H concentration in Pd increases with decreasing temperature. For example, when metallic Pd is exposed in a  $\text{H}_2$  pressure of 0.1 MPa at  $T = 300$  K, the H concentration in Pd is  $x \sim 0.7$ . As the temperature is lowered to  $T = 200$  K, the equilibrium concentration is expected to increase to  $x \sim 0.8$  from the extrapolation, which is larger than the critical concentration for superconductivity in  $\text{PdH}_x$ . Indeed, Akiba et al., prepared  $\text{PdH}_{0.83}$  even at  $\text{H}_2$  gas pressure of  $P \sim 0.1$  MPa, as long as the absorption was conducted at  $T = 210$  K, and succeeded with in-situ heat capacity experiments.<sup>94)</sup> Their results suggest that a highly concentrated H sample exhibiting superconductivity can be readily obtained. Stimulated by their results, we prepared highly concentrated  $\text{PdH}(\text{D})_x$ , where the charging was performed below 200 K and observed the superconducting transition through in-situ magnetization measurements down to  $T = 0.5$  K.<sup>92,93)</sup> In the following section, we describe the experimental procedure of the low-temperature absorption briefly. Then, we report our recent experiments on  $\text{PdH}_x$  and  $\text{PdD}_x$ .

#### 4.1 Hydrogen absorption in Pd

Pd metal powder with a particle diameter of 1–2  $\mu\text{m}$  and a purity of 99.95% was purchased from the Nilaco Corporation and was used for magnetization measurements. The magnetization was investigated down to a temperature of  $T = 0.5$  K using a home-made  $^3\text{He}$  insert attached to a Quantum Design MPMS SQUID magnetometer.<sup>95,96)</sup> After several activation processes by loading and evacuating  $\text{H}_2$  gas at  $T = 350$  K to remove the surface contamination, the Pd sample was cooled down to a temperature of  $T = 200, 150$ , or 120 K, at which the H absorption was performed. Next,  $\text{H}_2$  gas, which was stored in a reference volume, was introduced into the sample space. Owing to the H absorption of the Pd sample, the pressure  $P(t)$  of the gas handling system and sample space decreased rapidly with time  $t$ . Figure 3 illustrates the time evolution of the H concentration  $x$  and the magnetic susceptibility  $\chi$  in the Pd sample at  $T = 150$  K. After introducing  $\text{H}_2$  gas with an initial pressure of  $P_{\text{ini}} \sim 0.2$  MPa into the system, the H concentration  $x$  increases steeply, where  $x$  is estimated using the pressure change of the system with the Sievelts method.<sup>12)</sup> The absorption speed at  $T = 150$  K is about 10 times slower than that at  $T = 200$  K, indicating that the absorption of H atoms into the Pd sample and the diffusion are mainly governed by a thermal hopping process.<sup>97,98)</sup>

At the same time, the dc magnetic susceptibility  $\chi$  is measured under a magnetic field of  $H = 1000$  Oe to explore the H concentration dependence of  $\chi$  in Pd. It is well known that Pd is a metal close to the ferromagnetic state with a large paramagnetic susceptibility. In the present sample, a large  $\chi$  value of  $5.4 \times 10^{-4}$  emu/mol is observed at  $T = 150$  K.<sup>99–102)</sup> With increasing  $x$ , the susceptibility  $\chi$  decreases

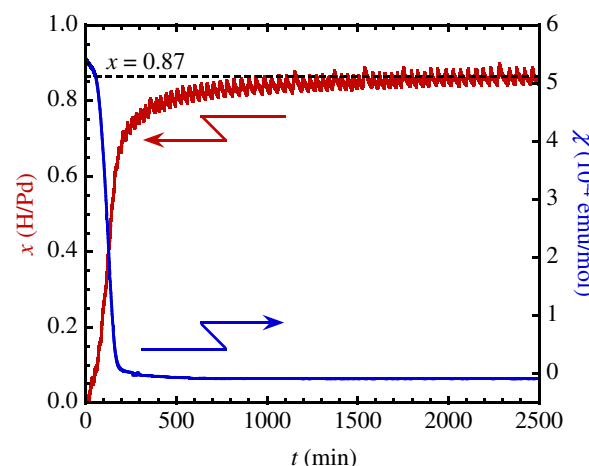


**Fig. 3.** (Color online) Time evolution of H concentration  $x$  and magnetic susceptibility  $\chi$ , which is measured under a magnetic field of  $H = 1000$  Oe in the Pd sample at 150 K, measured simultaneously. The concentration at  $t = 2600$  min is estimated to be  $x = 0.87$  from the pressure change of the system.

rapidly, as shown in Fig. 3. This means that  $\chi$  of the  $\alpha$ - $\beta$  mixed phase exhibits a strong suppression with  $x$  whereas  $\chi$  in the pure  $\beta$  phase is estimated to be  $0.15 \times 10^{-6}$  emu/g.<sup>49)</sup> When  $\chi$  is close to the boundary between the mixed phase and the pure  $\beta$  phase, the increase of  $x$  slows. This indicates a long relaxation time for H absorption and diffusion in the  $\beta$  phase owing to a repulsive interaction between the concentrated H atoms. Finally, the susceptibility is negative.

Looking closely at  $\chi$ , the initial slope for  $t \leq 70$  min is smaller than that of  $70 \leq t \leq 150$  min. This originates from the change in H absorption speed at the subsurface layer. In the H absorption process, H atoms expand Pd lattice, whereas a large potential barrier exists at the subsurface layer, which prevents the initial stage of H absorption.<sup>103)</sup>

#### 4.2 Superconducting properties in $\text{PdH}_x$

As illustrated in Fig. 3,  $\chi$  is almost a constant in the  $\beta$  phase, whereas a gradual increase of  $x$  is seen, which implies a long relaxation time until an equilibrium concentration is reached. At  $t = 2600$  min, H concentration was increased to  $x = 0.87$ . After cooling the insert to  $T = 25$  K to quench H in Pd, the remaining  $\text{H}_2$  gas was extracted and  $^3\text{He}$  gas was filled into the insert. Figure 4(a) displays the temperature dependence of the magnetization at several magnetic fields at  $x = 0.87$  down to  $T = 0.5$  K. Here, the sample temperature above  $T = 2$  K is controlled by the MPMS magnetometer using  $^3\text{He}$  as heat exchange gas in the insert. The temperature below 2 K is generated by pumping liquid  $^3\text{He}$ .

At  $H = 25$  Oe,  $M(T)$  starts to decrease due to diamagnetization arising from the superconducting transition at around  $T = 2.52$  K, which is assigned as  $T_c$ . By lowering the temperature,  $M(T)$  drops sharply and reaches almost a constant value at around 2 K. The width of the superconducting transition is about 0.5 K, which is sharp in comparison with previous results reached by other preparation methods. With increasing the magnetic field from 25 to 1500 Oe,  $T_c$  decreases monotonously.

At the lowest temperature  $T = 0.5$  K, the magnetic field dependence of the magnetization  $M(H)$  is recorded as shown in Fig. 4(b). Initially,  $M(H)$  curve decreases steeply up to

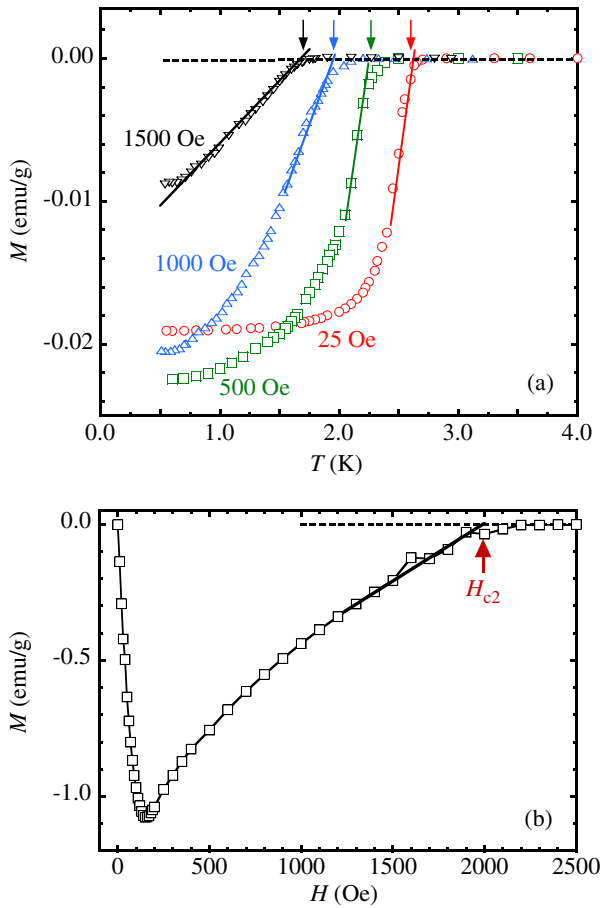


**Fig. 4.** (Color online) (a) Temperature dependence of the magnetization  $M(T)$  of  $\text{PdH}_{0.87}$  under various magnetic fields. The fields were applied at  $T = 10$  K, which is higher than  $T_c$ . (b) The field dependence of  $M(H)$  of  $\text{PdH}_{0.87}$  at 0.5 K, which was measured after zero field cooling.

150 Oe, and above 150 Oe,  $M(H)$  increases gradually to zero magnetization. These behaviors are characteristic for type II superconductors. The lower and upper critical fields are  $H_{c1} \sim 150$  Oe and  $H_{c2} \sim 2000$  Oe, which are determined at a peak field and an intersection field with zero magnetization, respectively.

Here, we discuss the sample quality prepared by the low-temperature absorption. In Fig. 5, the magnetic field dependence of  $M(H)$  is plotted for  $x = 0.82, 0.87$ , and  $0.91$ , which are prepared at an absorption temperature of  $T = 200, 150$ , and  $120$  K, respectively. The initial slope of the diamagnetization caused by the superconductivity is almost the same for all three samples, implying that they have similar superconducting properties. For a quantitative comparison, we estimate a superconducting volume fraction  $V_f$ , where  $V_f = -4\pi M_v/H$  and  $M_v$  is the magnetization per volume. To calculate  $V_f$ , the volume expansion caused by H absorption must be considered. In the case of octahedral site occupancy in Pd with fcc structure, the H-induced volume expansion  $v_H$  is given by the following relation. Up to  $x = 0.7$ ,  $v_H$  increases linearly with the formula  $2.8x \text{ \AA}^3$  and thereafter bends off with  $0.5(\pm 0.2)x \text{ \AA}^3$  for  $x > 0.7$ .<sup>104–108</sup> Consequently, the volume expansion for  $x = 0.82, 0.87$ , and  $0.91$  is estimated to be 11.3, 12.3, and 12.7%, respectively.

We plotted the magnetization per volume  $M_v$  for three concentrations, correcting the expansion, in the inset of Fig. 5. For the estimation, a demagnetizing factor of  $1/3$  is

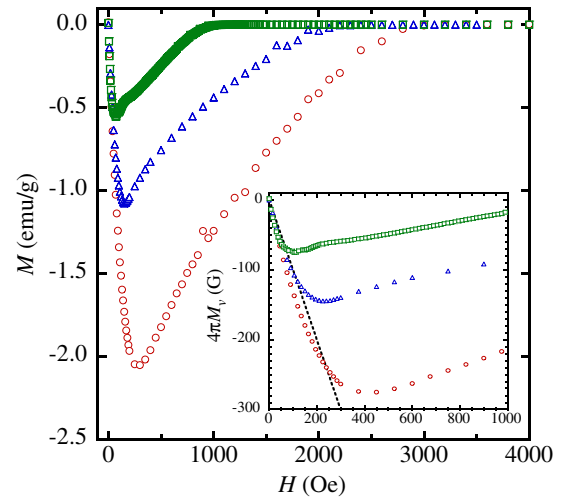


**Fig. 5.** (Color online) The magnetization  $M(H)$  is depicted as a function of the magnetic field for  $x = 0.82$  (squares),  $0.87$  (triangles), and  $0.91$  (circles). The inset shows the initial decrease of  $M(H)$  enlarged, where the vertical axis is plotted in  $4\pi M_v$ . The dotted line indicates perfect diamagnetism with a volume fraction of  $V_f = 1$ .

considered, by assuming a spherical shape of the powder sample. From a linear slope of  $M_v$  in the initial magnetic field range, the slope is slightly larger than  $V_f = 1$  for the three systems. Because for perfect diamagnetism  $V_f = 1$ , the diamagnetization value is clearly overestimated. The residual magnetic field in the superconducting magnet is the most probable origin for the overestimation. Additionally, the deviation of the demagnetizing factor due to non-uniformity of the sample powder should be considered as another origin of the overestimation. The sharp change of  $M(T)$  below  $T_c$  in Fig. 4(a) is well explained by assuming that  $V_f$  is close to unity. From these facts, we conclude that H atoms are absorbed into the Pd samples uniformly although the absorption was performed at low temperatures.

From  $M(T)$  and  $M(H)$  measurements, we describe the phase diagram as shown in Fig. 6. The magnetic field dependence of the transition temperature,  $T_c(H)$ , is reproduced by the empirical equation  $T_c(H) = T_c(0)(1 - H/H_{c2})^{1/\alpha}$  with  $\alpha = 2.78, 2.78$ , and  $2.0$  for  $x = 0.82, 0.87$ , and  $0.91$ , respectively, as drawn by the dashed curves. The transition temperature at zero field,  $T_c(0)$ , is estimated to be 1.35, 2.60, and 3.60 K by extrapolating the  $T_c(H)$  curve to  $H = 0$ . Because the relation between the transition temperature and the H concentration is given by  $T_c(0) = 150.8(x - 0.715)^{2.244}$ , as presented in Sect. 3.1,<sup>39</sup>  $x$  for the three samples is estimated to be 0.837, 0.879, and 0.904, respectively, which are in reasonable agreement with the evaluation based on the pressure change.

The upper critical field  $T_c(H)$  is increased with  $T_c$  at zero field, and the critical fields at  $T = 0$  K are  $H_{c2}(0) = 923, 2200$ , and  $2850$  Oe, respectively. These features are consistent with conventional superconductors. In contrast, previous results reported that  $T_c(H)$  in  $\text{PdH}_x$  was not only independent of  $T_c$  at zero field, but also linearly increased with decreasing temperature.<sup>23,25</sup> In these studies,  $T_c(H)$  was determined by resistivity measurements of  $\text{PdH}_x$  prepared by the electrochemical charging, which causes a broadening of the transition due to the inhomogeneity of the H concentration. As a result, the phase diagram might be modified

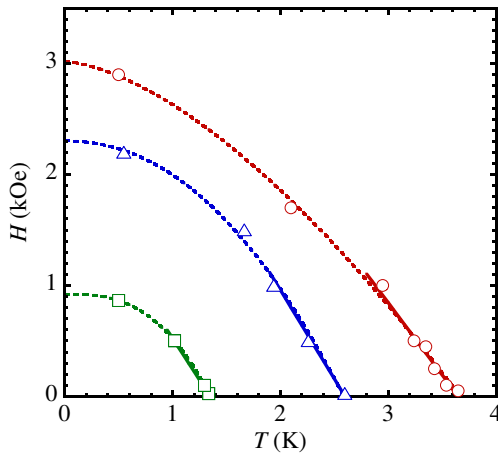


**Fig. 6.** (Color online) Phase diagram for  $\text{PdH}_x$  for  $x = 0.82$  (squares),  $0.87$  (triangles), and  $0.91$  (circles), where dashed lines are fits using a formula given in the text. Initial slopes of the phase boundaries near  $T_c(0)$ ,  $(dH_{c2}/dT)_{T_c}$  are indicated by solid lines.

largely. We consider that the concentration dependence of the phase diagram also provides another evidence that H atoms are absorbed uniformly into the Pd sample powder.

Theoretically, the upper critical field is determined by a combination of two different types of pair-breaking effects, i.e., the Pauli paramagnetic and orbital effects. The critical field predicted by the Pauli paramagnetic effect is given by  $H_p = 18400T_c(0)$ , which is much larger than  $H_{c2}(0)$  determined in the present results. Accordingly,  $H_{c2}$  is mainly governed by the orbital effect. In the vicinity of  $H = 0$ , the  $T_c(H)$  curves exhibit linear temperature dependences, and a Ginzburg–Landau (GL) theory for a type-II superconductor is utilized for the analysis. From the initial slope of  $H_{c2}$  at  $T = T_c(0)$ , we can estimate the orbital pair-breaking field using the formula  $H_{c2}^{\text{orb}}(0) = -0.69T_c(dH_{c2}/dT)_{T_c}$  as shown by Helfand and Werthamer.<sup>109</sup> In the present case,  $(dH_{c2}/dT)_{T_c} \sim -1500, -1600$ , and  $-1300 \text{ Oe/K}$  as illustrated by solid lines in Fig. 6, giving  $H_{c2}^{\text{orb}}(0) \sim 1400, 2870$ , and  $3230 \text{ Oe}$ , respectively. Using these values, the GL coherence length  $\xi(T)(0)$  at  $T = 0 \text{ K}$  is estimated to be  $48.5, 33.9$ , and  $31.9 \text{ nm}$  from the relation  $H_{c2}^{\text{orb}}(0) = \Phi_0/2\pi\xi^2(0)$ , where  $\Phi_0 = 2.07 \times 10^{-7} \text{ G/cm}^2$ . It should be noted that  $H_{c2}^{\text{orb}}(0)$  is nearly one and a half times larger the observed  $H_{c2}(0)$ , indicating the involvement of the paramagnetic and spin–orbit effects in the pair breaking.<sup>110</sup>

#### 4.3 Resistivity measurements of $\text{PdH}_x$

Synthesis of  $\text{PdH}_x$  thin films enables a variety of experiments such as the tunnel junction investigation. In previous experiments, H charging in the thin film was done under special experimental conditions.<sup>58–60</sup> As presented above, the low-temperature H absorption is performed in a gentle condition, simplifying the experimental procedure. Thus, using this method  $\text{PdH}_x$  thin film may be synthesized without breaking the film due to the lattice expansion caused by H absorption.

A Pd film with a thickness of  $\sim 100 \text{ nm}$  was prepared by magnetron sputtering under a base pressure of  $2 \times 10^{-6} \text{ Pa}$ . Then, the Cu electrical pads were formed by the thermal evaporation. H absorption into the film was performed in the same manner as that used for the Pd powder in preparation

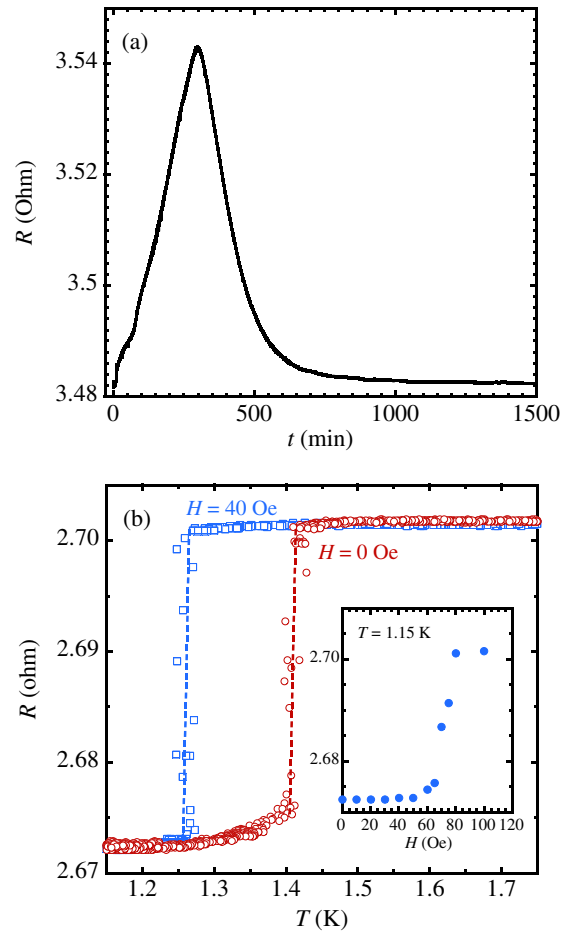


**Fig. 7.** (Color online) (a) Time evolution of the resistance for the Pd film exposed in  $\text{H}_2$  gas with an initial pressure of  $P_{\text{ini}} = 0.22 \text{ MPa}$ . By comparison to previous resistance measurements in  $\text{PdH}_x$  film,<sup>32,111,112</sup> the H concentration is expected to be larger than  $x = 0.8$ . (b) Temperature dependence of the resistance in the Pd–H film, which shows a resistance drop due to the superconducting transition at around  $1.42$  and  $1.25 \text{ K}$  in  $H = 0$  and  $40 \text{ Oe}$ , respectively. Inset shows the magnetic field dependence of the resistance.

for the magnetization measurements, shown in Fig. 3. At  $200 \text{ K}$ ,  $\text{H}_2$  gas at an initial pressure of  $P_{\text{ini}} = 0.22 \text{ MPa}$  was introduced into the  $^3\text{He}$  insert mounting the Pd film. In the present experiments, the H concentration in the film cannot be estimated by the Sievelts method due to the small amount of Pd mass. Therefore, we predicted the H concentration by the concentration dependence of the resistance in the Pd film.<sup>111</sup> In Fig. 7(a), we show the time evolution of the resistance in the Pd film, which is measured by a LR700 resistance bridge. After introducing  $\text{H}_2$  gas into the insert, the resistance increases steeply and shows a maximum, which is followed by a sharp drop. Finally, the resistance becomes almost constant. These features are in good agreement with the H concentration dependence of the resistance in  $\text{PdH}_x$  prepared by gas loading at high pressure<sup>111,112</sup> and electrochemical loading,<sup>113</sup> where the maximum is observed at  $x \sim 0.75$  in the room temperature measurements. Moreover, the maximum at  $x \sim 0.75$  is also confirmed at  $4.2 \text{ K}$ . From these results, we expected the concentration of the Pd film to be larger than  $x = 0.8$ .

After the process described above, we decreased the temperature of the insert to  $25 \text{ K}$  and evacuated the  $\text{H}_2$  gas.



Subsequently,  $^3\text{He}$  gas is introduced into the insert. We display the temperature dependence of the resistance in Fig. 7(b). The resistance drop due to the superconducting transition is seen at around  $T_c = 1.42$  K. Note that the resistance does not vanish despite finishing the transition, which is caused by resistance of the Cu pad.  $T_c$  observed in the Pd film is slightly higher than the  $T_c(0) \sim 1.35$  K in  $\text{PdH}_{0.82}$  powders, which probably originates from the difference of the initial pressure for the H absorption. The H charging in powders at  $T = 200$  K is performed at  $P_{\text{ini}} = 0.185$  MPa, whereas that in the film is performed at  $P_{\text{ini}} = 0.22$  MPa. These suggest that  $T_c$  can be controlled precisely by changing the initial pressure of the  $\text{H}_2$  gas. At  $H = 40$  Oe, the transition temperature is suppressed to  $T_c \sim 1.25$  K. From these results, we conclude that the low-temperature H absorption is utilized for synthesizing the superconducting  $\text{PdH}_x$  film. In contrast, the critical field is observed to be  $H = 70$  Oe, as plotted in the inset, which is much smaller than that seen in the magnetization measurements. This suggests that cracks are produced by the expansion caused by the H absorption, which then depresses the critical current of the Pd film.

#### 4.4 Deuterium absorption experiments

Finally, we present D absorption experiments in Pd powders. The experimental procedure is the same as for  $\text{PdH}_x$  case. Figure 8 displays the evolution of the D concentration  $x (= \text{D}/\text{Pd})$  in Pd, which was carried out at an initial pressure of  $P_{\text{ini}} = 0.327$  MPa at  $T = 200$  K. The absorption process and magnetic susceptibility  $\chi$  are recorded simultaneously. At first glance, the whole feature of the absorption process is similar to that of  $\text{PdH}_x$  shown in Fig. 3. As shown by a solid line in the inset, the initial slope of  $\chi$  below 5 min is slightly smaller than that above 5 min, reflecting a slowing down of the D absorption at the subsurface layer as in the case of H absorption. When  $\chi$  approaches the diamagnetic region, the increase of  $x$  is suppressed, indicating a long relaxation time for the D absorption and diffusion in the pure  $\beta$  phase. The absorption is slower compared to that in  $\text{PdH}_x$  at  $T = 200$  K because of the mass difference,<sup>92</sup> indicating that preparing a highly concentrated D system with this method would be difficult.<sup>114</sup> The switch from paramagnetic to diamagnetic occurs at around  $x_\beta = 0.58$ , which is smaller than that in the H system and agrees with the previously reported value.<sup>115,116</sup> Finally, a D concentration of  $x = 0.79$  was obtained.

$M(T)$  and  $M(H)$  measured for  $\text{PdD}_{0.79}$  are plotted in Figs. 9(a) and 9(b), respectively. The qualitative features of the superconducting properties of  $\text{PdD}_{0.79}$  are similar to those of  $\text{PdH}_x$ . With increasing magnetic field,  $T_c$  is suppressed monotonously from 1.23 K at 25 Oe to 0.75 K at 750 Oe, as shown in  $M(T)$  curve. From the  $M(H)$  curve, it can be seen that the lower and upper critical fields at  $T = 0.5$  K are at  $H_{c1} = 40$  Oe and  $H_{c2} = 880$  Oe, respectively. The magnetic field dependence of the transition temperature,  $T_c(H)$ , was well reproduced by the empirical equation  $T_c(H) = T_c(0)(1 - H/H_{c2})^{1/\alpha}$  where  $\alpha = 3.10$ . From this relation, the transition temperature at zero field and the upper critical field at  $T = 0$  K were estimated to be  $T_c(0) = 1.22$  K and  $H_{c2}(0) = 940$  Oe, respectively. Although  $T_c(0)$  of  $\text{PdD}_{0.79}$  is lower than that of  $\text{PdH}_{0.82}$ ,  $H_{c2}(0)$  is expected to be higher

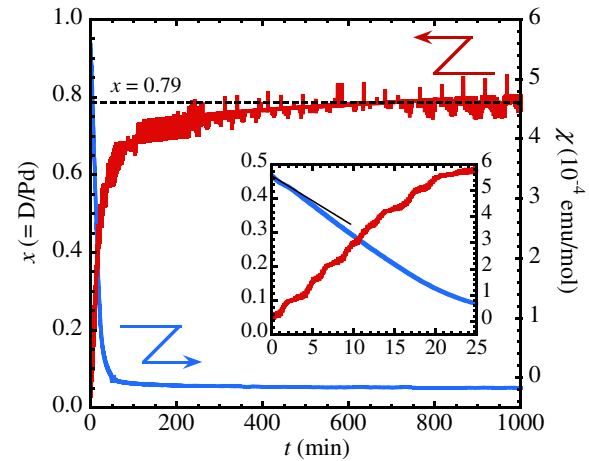


**Fig. 8.** (Color online) Time evolution of  $x$  and magnetic susceptibility  $\chi$  at 200 K, which are measured simultaneously. The D concentration was estimated to be  $x = 0.79$  from the pressure change of the system using the Sievelts method.<sup>12)</sup> The inset shows a close-up of the initial evolution of  $\chi$  and  $x$ , where the initial slope of  $\chi$  is fitted by a solid line.

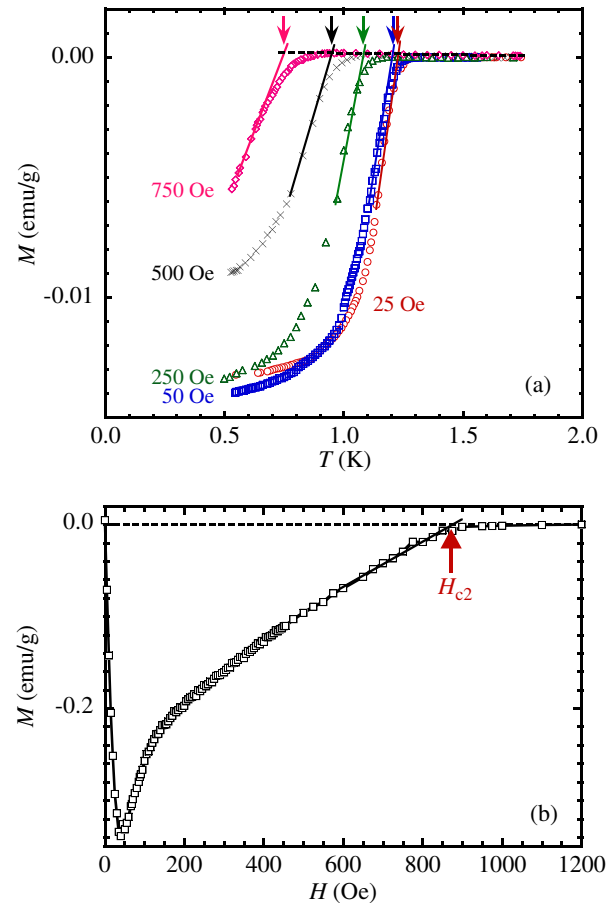


**Fig. 9.** (Color online) (a)  $M(T)$  of  $\text{PdD}_{0.79}$  under various magnetic fields, where the fields were applied at  $T = 10$  K. (b)  $M(H)$  curve of  $\text{PdD}_{0.79}$  at  $T = 0.5$  K, which was cooled in zero field.

than for  $\text{PdH}_{0.82}$ . This can be caused by the inverse isotope effect. The superconducting volume fraction was estimated to be  $V_f \sim 1$ , indicating that D atoms are absorbed uniformly, as in the case of H atoms. Moreover, the superconducting coherence length in  $\text{PdH}_{0.82}$  was calculated to be 48.0 nm.<sup>92)</sup>

## 5. Conclusion

In this paper, we present an overview of the experimental investigations on the superconducting properties of  $\text{PdH}_x$  and  $\text{PdD}_x$ . First, we introduce methods for H loading into Pd, in which three principal techniques, i.e., gas loading, electrochemical loading, and H implantation are introduced, and then the superconducting properties of  $\text{PdH}_x$  and  $\text{PdD}_x$  studied so far are briefly summarized. Next, we describe our recent in-situ magnetization measurements of superconducting  $\text{PdH}_x$  and  $\text{PdD}_x$  powders and the resistance measurements of a  $\text{PdH}_x$  thin film, where H charging is done under a  $\text{H}_2$  and  $\text{D}_2$  gas atmosphere below 200 K. All systems exhibit superconducting transitions. From  $M(T)$  and  $M(H)$  measurements, we estimate the superconducting volume fraction and describe the  $T$ – $H$  phase diagram, implying that H or D atoms are absorbed uniformly in the sample. From these results, we conclude that the experimental procedure combining the low-temperature absorption with in-situ measurements provides a new way to reveal the intrinsic nature of superconductivity in  $\text{PdH(D)}_x$  systems.

**Acknowledgments** We specially thank to Professor Yamamuro for giving information about the low-temperature H absorption into Pd, which inspires the present study. We also thank to Mrs. Hasuo and Yamaguchi for their technical help. This work was supported by JSPS KAKENHI Grant Numbers, JP18K04683, JP15K06424, 26600102, 25220605, 25287076, JSPS Program for Fostering Globally Talented Researchers, Grant Number JPMXS05R2900005, and Iketani Science and Technology Foundation.

\*t.kawae.122@m.kyushu-u.ac.jp

- 1) A. P. Drozdov, M. I. Erements, I. A. Troyan, V. Ksenofontov, and S. I. Shylin, *Nature* **525**, 73 (2015).
- 2) M. Somayazulu, M. Ahart, A. K. Mishra, Z. M. Geballe, M. Baldini, Y. Meng, V. V. Struzhkin, and R. J. Hemley, *Phys. Rev. Lett.* **122**, 027001 (2019).
- 3) H. Liu, I. I. Naumov, R. Hoffmann, N. W. Ashcroft, and R. J. Hemley, *Proc. Natl. Acad. Sci. U.S.A.* **114**, 6990 (2017), and the references are therein.
- 4) F. H. Horn and W. T. Ziegler, *J. Am. Chem. Soc.* **69**, 2762 (1947).
- 5) C. B. Satterthwaite and I. L. Toepke, *Phys. Rev. Lett.* **25**, 741 (1970).
- 6) T. Skoskiewicz, *Phys. Status Solidi A* **11**, K123 (1972).
- 7) F. A. Lewis, *The Palladium–Hydrogen System* (Academic Press, New York, 1967).
- 8) F. D. Manchester, A. San-Martin, and J. M. Pitre, *J. Phase Equilibria* **15**, 62 (1994).
- 9) J. E. Schirber, *Phys. Lett. A* **46**, 285 (1973).
- 10) J. E. Schirber and C. J. M. Northrup, Jr., *Phys. Rev. B* **10**, 3818 (1974).
- 11) J. E. Schirber, J. M. Mintz, and W. Wall, *Solid State Commun.* **52**, 837 (1984).
- 12) T. P. Blach and E. MacA. Gray, *J. Alloys Compd.* **446–447**, 692 (2007).
- 13) T. Skoskiewicz, A. A. Szafranski, W. Bujnowski, and B. Baranowski, *J. Phys. C* **7**, 2670 (1974).
- 14) I. S. Balbaa and F. D. Manchester, *J. Phys. F* **13**, 395 (1983).
- 15) I. S. Balbaa, A. J. Pindor, and F. D. Manchester, *J. Phys. F* **14**, 2637 (1984).
- 16) T. Skoskiewicz, M. Horobiowski, and E. Trojnar, *J. Less-Common Met.* **101**, 311 (1984).
- 17) J. E. Schirber, *Phys. Lett. A* **45**, 141 (1973).
- 18) T. Skoskiewicz, A. W. Szafranski, and B. Baranowski, *Phys. Status Solidi B* **59**, K135 (1973).
- 19) R. Wisniewski and A. J. Rostocki, *Phys. Rev. B* **3**, 251 (1971).
- 20) H. Hemmes, A. Driessen, R. Griessen, and M. Gupta, *Phys. Rev. B* **39**, 4110 (1989).
- 21) H. Hemmes, A. Driessen, J. Rector, and R. Griessen, *J. Phys.: Condens. Matter* **1**, 8123 (1989).
- 22) H. Hemmes, A. Driessen, J. Kos, F. A. Mul, R. Griessen, J. Caro, and S. Radelaar, *Rev. Sci. Instrum.* **60**, 474 (1989).
- 23) T. Skoskiewicz, *Phys. Status Solidi B* **59**, 329 (1973).
- 24) W. Buckel, A. Eichler, and B. Stritzker, *Z. Phys.* **263**, 1 (1973).
- 25) N. E. Alekseevskii, Yu. A. Samarskii, H. Wolf, V. I. Tsebro, and V. M. Zakosarenko, *JETP Lett.* **19**, 350 (1974).
- 26) C. A. Mackliet, D. J. Gillespie, and A. I. Schindler, *Solid State Commun.* **15**, 207 (1974).
- 27) C. A. Mackliet, D. J. Gillespie, and A. I. Schinder, *J. Phys. Chem. Solids* **37**, 379 (1976).
- 28) J. P. Burger, D. S. McLachlan, R. Mailfert, and B. Souffache, *Solid State Commun.* **17**, 277 (1975).
- 29) D. S. MacLachlan, R. Mailfert, J. P. Burger, and B. Souffaché, *Solid State Commun.* **17**, 281 (1975).
- 30) G. J. Zimmermann, *J. Less-Common Met.* **49**, 49 (1976).
- 31) D. S. McLachlan and T. B. Doyle, *J. Low Temp. Phys.* **26**, 590 (1977).
- 32) T. F. Smith and G. K. White, *J. Phys. F* **7**, 1029 (1977).
- 33) J. M. E. Harper, *Phys. Lett. A* **47**, 69 (1974).
- 34) R. J. Miller and C. B. Satterthwaite, *Phys. Rev. Lett.* **34**, 144 (1975).
- 35) M. Zimmermann, G. Wolf, and K. Bohmhammel, *Phys. Status Solidi A* **31**, 511 (1975).
- 36) F. Antonangeli, A. Balzarotti, A. Bianconi, P. Perfetti, P. Ascarelli, and N. Nistico, *Solid State Commun.* **21**, 201 (1977).
- 37) C. L. Wiley and F. Y. Fradin, *Phys. Rev. B* **17**, 3462 (1978).
- 38) D. R. Krahn, R. L. Henryd, D. B. Tanner, and P. E. Wigen, *Phys. Status Solidi A* **46**, 209 (1978).
- 39) R. W. Standley, M. Steinback, and C. B. Satterthwaite, *Solid State Commun.* **31**, 801 (1979).
- 40) S. Yasuzuka, N. Ogita, D. Anzai, and N. Hatakenaka, *J. Phys. Soc. Jpn.* **85**, 123703 (2016).
- 41) B. Stritzker and W. Buckel, *Z. Phys.* **257**, 1 (1972).
- 42) W. Buckel and B. Stritzker, *Phys. Lett. A* **43**, 403 (1973).
- 43) B. Stritzker, *Z. Phys.* **268**, 261 (1974).
- 44) G. Heim and B. Stritzker, *Appl. Phys.* **7**, 239 (1975).
- 45) B. Stritzker, *J. Nucl. Mater.* **72**, 256 (1978).
- 46) A. Leiberich, W. Scholz, and W. J. Standish, *Phys. Lett. A* **87**, 57 (1981).
- 47) B. Stritzker and H. Wuhl, in *Hydrogen in Metals II*, ed. G. Alefeld and J. Volkl (Springer, New York, 1978).
- 48) K. H. Bennemann and J. W. Garland, *Z. Phys.* **260**, 367 (1973).
- 49) H. C. Jamieson and F. D. Manchester, *J. Phys. F* **2**, 323 (1972).
- 50) E. Matsushita, *Solid State Commun.* **38**, 419 (1981).
- 51) S. Auluck, *Lett. Nuovo Cimento* **7**, 545 (1973).
- 52) U. Mizutani, T. B. Massalski, and J. Bevk, *J. Phys. F* **6**, 1 (1976).
- 53) J. M. Rowe, J. J. Rush, H. G. Smith, M. Mostoller, and H. E. Flotow, *Phys. Rev. Lett.* **33**, 1297 (1974).
- 54) R. Abbenseth and H. Wipf, *J. Phys. F* **10**, 353 (1980).
- 55) A. Rahman, K. Skold, C. Pelizzari, S. K. Sinha, and H. Flotow, *Phys. Rev. B* **14**, 3630 (1976).
- 56) C. J. Glinka, J. M. Rowe, J. J. Rush, A. Rahman, S. K. Sinha, and H. E. Flotow, *Phys. Rev. B* **17**, 488 (1978).
- 57) B. N. Ganguly, *Z. Phys.* **265**, 433 (1973).
- 58) A. Eichler, H. Wuhl, and B. Stritzker, *Solid State Commun.* **17**, 213 (1975).
- 59) P. J. Silverman and C. V. Briscoe, *Phys. Lett. A* **53**, 221 (1975).
- 60) J. Igalson, L. Sniadower, A. J. Pindor, T. Skoskiewicz, K. Bliithner, and F. Dettmann, *Solid State Commun.* **17**, 309 (1975).
- 61) P. Nedellec, L. Dumoulin, and J. P. Burger, in *Electronic Structure and Properties of Hydrogen in Metals*, ed. P. Jena and C. B. Satterthwaite (Plenum, New York, 1983) p. 347.
- 62) B. Stritzker and J. Becker, *Phys. Lett. A* **51**, 147 (1975).
- 63) B. Stritzker and H. L. Luo, *J. Less-Common Met.* **73**, 301 (1980).
- 64) B. Stritzker and H. L. Luo, *Solid State Commun.* **29**, 811 (1979).
- 65) T. Skoskiewicz, *Phys. Status Solidi A* **48**, K165 (1978).
- 66) G. Wolf and C. Hohlfeld, *Phys. Status Solidi A* **36**, K99 (1976).
- 67) G. Wolf, J. Jahnke, and K. Bohmhammel, *Phys. Status Solidi A* **36**, K125 (1976).
- 68) A. W. Szafranski, T. Skoskiewicz, and B. Baranowski, *Phys. Status Solidi A* **37**, K163 (1976).
- 69) V. E. Antonov, T. E. Antonova, T. Beleash, E. G. Ponyatovskii, and V. I. Rasiupkin, *Phys. Status Solidi A* **78**, 137 (1983).
- 70) C. G. Robbins and J. Muller, *J. Less-Common Met.* **42**, 19 (1975).

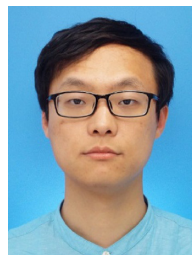
- 71) C. B. Friedberg, A. F. Rex, and J. Ruvalds, *Phys. Rev. B* **19**, 5694 (1979).
- 72) A. A. Abrikosov, *Sov. Phys. JETP* **14**, 408 (1962).
- 73) N. W. Ashcroft, *Phys. Rev. Lett.* **21**, 1748 (1968).
- 74) T. Schneider and E. Stoll, *Physica* **55**, 702 (1971).
- 75) P. Hertel, *Z. Phys.* **268**, 111 (1974).
- 76) J. S. Brown, *Phys. Lett. A* **51**, 99 (1975).
- 77) B. N. Ganguly, *Phys. Rev. B* **14**, 3848 (1976).
- 78) D. A. Papaconstantopoulos and B. M. Klein, *Phys. Rev. Lett.* **35**, 110 (1975).
- 79) A. J. Pindor, *Phys. Status Solidi B* **74**, K19 (1976).
- 80) T. Nakajima, *Phys. Status Solidi B* **77**, K147 (1976).
- 81) J. P. Burger and D. S. McLachlan, *J. Phys. (Paris)* **37**, 1227 (1976).
- 82) B. N. Ganguly, *Z. Phys. B* **22**, 127 (1975).
- 83) B. M. Klein, E. N. Economou, and D. A. Papaconstantopoulos, *Phys. Rev. Lett.* **39**, 574 (1977).
- 84) P. Jena, C. L. Wiley, and F. Y. Fradin, *Phys. Rev. Lett.* **40**, 578 (1978).
- 85) J. P. Burger, *J. Less-Common Met.* **101**, 53 (1984).
- 86) P. Jena, J. Jones, and R. M. Nieminen, *Phys. Rev. B* **29**, 4140 (1984).
- 87) P. M. Laufer and D. A. Papaconstantopoulos, *Phys. Rev. B* **33**, 5134(R) (1986).
- 88) B. M. Klein and R. E. Cohen, *Phys. Rev. B* **45**, 12405 (1992).
- 89) M. Yussouff, B. K. Rao, and P. Jena, *Solid State Commun.* **94**, 549 (1995).
- 90) I. Errea, M. Calandra, and F. Mauri, *Phys. Rev. Lett.* **111**, 177002 (2013).
- 91) S. Villa-Cortés and R. Baquero, *J. Phys. Chem. Solids* **123**, 371 (2018).
- 92) Y. Inagaki, S. Wen, Y. Kawasaki, H. Takata, Y. Furukawa, and T. Kawae, *J. Phys. Soc. Jpn.* **87**, 123701 (2018).
- 93) Y. Inagaki, S. Wen, R. Hirota, Y. Furukawa, and T. Kawae, in preparation.
- 94) H. Akiba, H. Kobayashi, H. Kitagawa, M. Kofu, and O. Yamamuro, *Phys. Rev. B* **92**, 064202 (2015).
- 95) Y. Sato, S. Makiyama, Y. Sakamoto, T. Hasuo, Y. Inagaki, T. Fujiwara, J. S. Suzuki, K. Matsubayashi, Y. Uwatoko, and T. Kawae, *Jpn. J. Appl. Phys.* **52**, 106702 (2013).
- 96) T. Kawae, M. Koga, Y. Sato, S. Makiyama, Y. Inagaki, N. Tateiwa, T. Fujiwara, H. S. Suzuki, and T. Kitai, *J. Phys. Soc. Jpn.* **82**, 073701 (2013).
- 97) S. Majorowski and B. Baranowski, *J. Phys. Chem. Solids* **43**, 1119 (1982).
- 98) H. Okuyama, W. Siga, N. Takagi, M. Nishijima, and T. Aruga, *Surf. Sci.* **401**, 344 (1998).
- 99) F. E. Hoare and J. C. Matthews, *Proc. R. Soc. London, Ser. A* **212**, 137 (1952).
- 100) M. Shimizu, K. Kato, and T. Tsui, *Phys. Lett. A* **28**, 656 (1969).
- 101) H. Nagasawa, *J. Phys. Soc. Jpn.* **28**, 1171 (1970).
- 102) Y. Y. Chen, Y. D. Yao, S. U. Jen, B. T. Lin, H. M. Lin, C. Y. Tung, and S. S. Hsiao, *Nanostruct. Mater.* **6**, 605 (1995).
- 103) B. D. Kay, C. H. F. Peden, and D. W. Goodman, *Phys. Rev. B* **34**, 817 (1986).
- 104) R. Feenstra, R. Griessen, and D. G. de Groot, *J. Phys. F* **16**, 1933 (1986).
- 105) V. E. Antonov, M. Baier, B. Dörner, V. K. Fedotov, G. Grosse, A. I. Kolesnikov, E. G. Ponyatovsky, G. Schneider, and F. E. Wagner, *J. Phys.: Condens. Matter* **14**, 6427 (2002).
- 106) Y. Fukai, *Z. Phys. Chem.* **163**, 165 (1989).
- 107) J. E. Schirber and B. Morosin, *Phys. Rev. B* **12**, 117 (1975).
- 108) E. Wicke and H. Brodowsky, in *Topics in Applied Physics: Hydrogen in Metals II*, ed. A. Alefeld and J. Volkl (Springer, Berlin/Heidelberg, 1978) Vol. 29, Chap. 3.
- 109) E. Helfand and N. R. Werthamer, *Phys. Rev.* **147**, 288 (1966).
- 110) N. R. Werthamer, E. Helfand, and P. C. Hohenberg, *Phys. Rev.* **147**, 295 (1966).
- 111) R. Wisniewski and A. J. Bostock, *Phys. Rev. B* **3**, 251 (1971).
- 112) B. Baranowski and R. Wisniewski, *Phys. Status Solidi* **35**, 593 (1969).
- 113) R. S. Smith and D. A. Otterson, *J. Phys. Chem. Solids* **31**, 187 (1970).
- 114) F. A. Lewis, *Platin. Met. Rev.* **26**, 20 (1982).
- 115) E. Wicke and J. Blaurock, *J. Less-Common Met.* **130**, 351 (1987).
- 116) R. Lässer and K.-H. Klatt, *Phys. Rev. B* **28**, 748 (1983).



**Tatsuya Kawae** obtained his B.Sc. degree from Osaka City University in 1985 and Ph.D. degree from University of Tokyo in 1993. He worked as a research associate in Kyushu University from 1993 and currently as an associate professor. His research is focused on experimental low temperature physics.



**Yuji Inagaki** was born in Kobe, Japan in 1969. He obtained his D.Sc. degree from Kyushu University in 2003. He was a postdoc at Kobe and Kyushu University. Since 2006, he has been an assistant professor at Kyushu University. He is a Visiting Scholar at Ames Laboratory, Iowa State University and CEA-Grenoble. His research interests are in magnetism and hydrogen related phenomena.



**Si Wen** was born in Baoji, Shaanxi, China in 1994. He obtained a bachelor degree from XI' DIAN University in 2016 and a master degree from Kyushu University in 2019.



**Souhei Hirota** was born in Fukuoka in 1995. He was obtained a bachelor degree from Kyushu University and entered the master course in 2018.



**Daiki Ito** was born in Wakayama Prefecture, Japan in 1996. He obtained his B.Sc. (2018) degree from Shinshu University. He was master student in Kyushu University department of physics since 2018. He is interest in experimental study on spin dependent transports in the systems with strong spin-orbit interaction.



**Takashi Kimura** was born in Wakayama Prefecture, Japan in 1975. He obtained his B.Sc. (1997), M.Sc. (1999), and D.Sc. (2002) degrees from Osaka University. He was a Post-doctoral Fellowship in Riken, (2002–2004), Assistant Professor in University of Tokyo, (2005–2008), and a professor in Kyushu University since 2009. He is interested in experimental study on condensed matter physics, in particular spintronics in metallic nanostructures.